*Supplementary material for*

# Flower-like $Bi_{12}O_{17}Cl_2$/β-$Bi_2O_3$ heterojunction for photocatalytic wastewater purification

Tianyuan Xiao[a,1], Xinyue Dong[c,1], Yong Li[a], Xiaoya Ding[b*], Guangming Yin[a,c*]

a. College of Light Industry and Textiles, Qiqihar University, Qiqihar, China, 161006.
b. College of Architecture and Civil Engineering, Qiqihar University, Qiqihar, China, 161006.
c. Center for Analytical Testing, Qiqihar University, Qiqihar, China, 161006.
*Corresponding author: qdyingm@163.com, dxy03422@163.com

**Table. S1**

Table S1. The grain size of the characteristic diffraction peaks

| Materials | Hkl | FWHM | Grain size |
|---|---|---|---|
| $Bi_{12}O_{17}Cl_2$ | 117 | 0.332 | 24.5 nm |
| β-$Bi_2O_3$ | 222 | 0.243 | 35.2 nm |
| $Bi_{12}O_{17}Cl_2$(heterojunction) | 117 | 0.392 | 20.8 nm |
| β-$Bi_2O_3$(heterojunction) | 222 | 0.185 | 42.7 nm |

**S1 Raman spectrum**

In order to further confirm the crystal structure, the Raman spectra are necessary as these two phases have totally different Raman peaks. As for $Bi_{12}O_{17}Cl_2$/β-$Bi_2O_3$ material's characteristic peaks of the β-$Bi_2O_3$ and $Bi_{12}O_{17}Cl_2$ were present in the heterostructures. Fig. S1 reveals from the Raman spectra of the β-$Bi_2O_3$ that all the peaks located at 119, 311, 463 and 600 $cm^{-1}$ in the pattern of the sample grown were well assigned to the β-$Bi_2O_3$. In fact, this material displays the Raman band pattern of a typical $Bi_{12}O_{17}Cl_2$ compound with its main bands at 143, and a weak band at 377 $cm^{-1}$. These bands correspond to the $A_{1g}$ internal Bi-Cl stretching mode, $E_{1g}$ internal Bi-Cl stretching vibration. The Raman analysis further, confirmed the synthesis of $Bi_{12}O_{17}Cl_2$/β-$Bi_2O_3$ heterostructures.

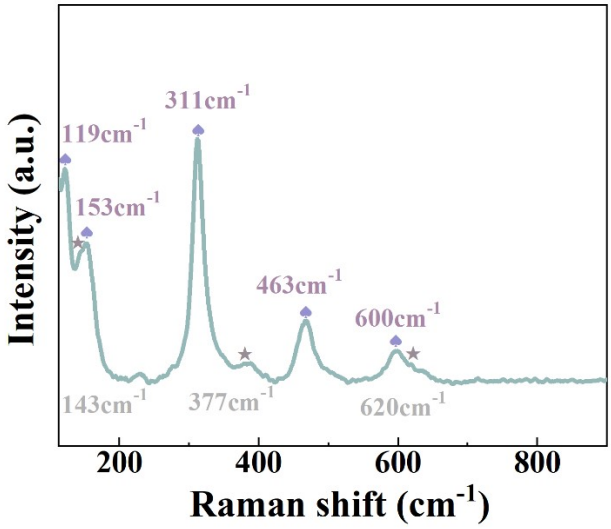


**Fig. S1.** Raman shift of particles.

**S2 TRPL measurements**

The average carrier lifetime of the Flower-like $Bi_{12}O_{17}Cl_2$/β-$Bi_2O_3$ heterojunction catalyst was τ=7.28 ns, which was obviously longer than that of the single-component $Bi_{12}O_{17}Cl_2$ (4.06 ns) and β-$Bi_2O_3$ (3.68 ns). The longer carrier lifetime indicates that the construction of the heterojunction effectively inhibits the recombination of photogenerated electron-hole pairs, which further proves that the heterojunction structure can optimize the photocatalytic performance of the material.

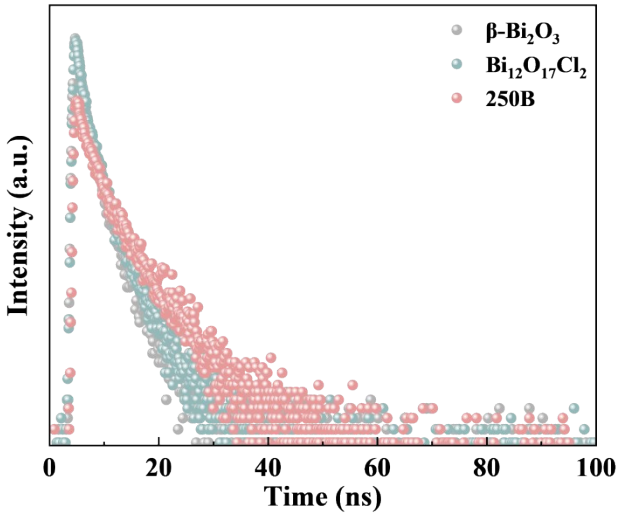


**Fig. S2.** TRPL signals.

**Table. S2**

Table S2. Photocatalysis degradation comparison with previous works

| Photocatalyst | pH | Catalyst loading | MB concentration | Degradation | Time (min) | Ref. |
|---|---|---|---|---|---|---|
| $GO/TiO_2/SiO_2$ | 10 | 0.3 g/L | 0.5 mg/L | 84.6% | 120 | 1 |
| Chlorophyll-$TiO_2$ | 6 | 2.5 g/L | 20 mg/L | 85% | 120 | 2 |
| $Cu_{2-x}Se$ NPs | 7 | 0.5 g/L | 10 mg/L | 90.3% | 90 | 3 |
| $MnTiO_3$ | 7 | 0.05 g/L | 15 mg/L | 75% | 240 | 4 |
| GO | 6.8 | 0.2 g/L | 25 mg/L | 99% | 60 | 5 |
| $g\text{-}C_3N_4/Fe_3O_4$ | 3 | 0.4 g/L | 20 mg/L | 90% | 90 | 6 |
| Au-$BiFeO_3$ | 7 | 0.15 g/L | 10 mg/L | 92% | 120 | 7 |
| N-$TiO_2$/CNT | 7 | 0.25 g/L | 20 mg/L | 94% | 90 | 8 |
| $Co_3O_4$/ZnO@ MG-$C_3N_x$ | 7 | 0.25 g/L | 12 mg/L | 89.5% | 120 | 9 |
| Commercial ZnO | 6.8 | 0.4 g/L | 12 mg/L | 85.7% | 60 | 10 |
| Our work | 6 | 0.04 g/L | 10 mg/L | 91.5% | 120 | |

**S3 ESR analysis**

Recognizing the significance of active radicals in photocatalytic wastewater purification, ESR spin-trap experiments using DMPO were conducted. Fig. S3 present the results, demonstrating that 250B did not show significant ESR signals of $\cdot O_2^-$ in the absence of light. However, under visible light exposure for 30 minutes, the photoexcitation of the 250B composite resulted in pronounced peaks of DMPO-$\cdot O_2^-$ and TEMPO-$h^+$, indicating the generation of $h^+$ and $\cdot O_2^-$ radicals. Comparing the signal peaks across the samples, it was observed that the signal intensities of the TEMPO- $h^+$ spin adduct were slightly stronger than those of $\cdot O_2^-$. The presence of active radicals in the $Bi_{12}O_{17}Cl_2$/β-$Bi_2O_3$ system was attributed to multiple electron transfer pathways at heterojunction interfaces and the exposure of active crystal planes.

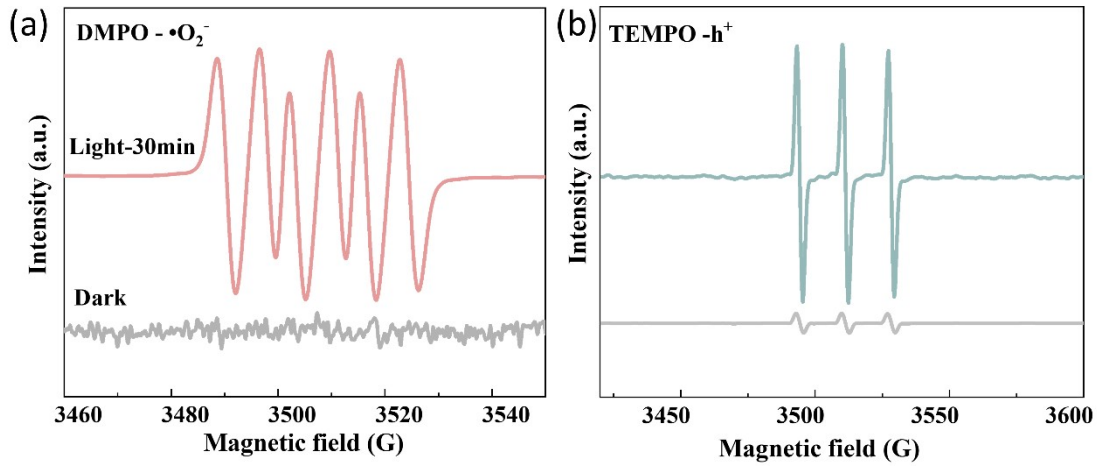


**Fig. S3.** (a) DMPO-$\cdot O_2^-$ and (b) TEMPO- $h^+$.

**References**

1. Zhou, Y., et al. A Comparative Study of $GO/TiO_2/SiO_2$ Catalysts for the Photocatalytic Degradation of Methylene Blue and Phenolic Compounds. Catalysts, (2025), 15(2), 289.

2. Krishnan, Sukanya, and Amritanshu Shriwastav. Application of $TiO_2$ nanoparticles sensitized with natural chlorophyll pigments as catalyst for visible light photocatalytic degradation of methylene blue. Journal of Environmental Chemical Engineering 9.1 (2021): 104699.

3. Patel, Pushpanjali, et al. Sunlight-driven catalytic degradation of MB dye and multi-cycle Re-usability analysis of $Cu_{2-x}Se$ nanoparticles. Heliyon 10.21 (2024).

4. Alkaykh, Suhila, Aïcha Mbarek, and Elbashir E. Ali-Shattle. Photocatalytic degradation of methylene blue dye in aqueous solution by $MnTiO_3$ nanoparticles under sunlight irradiation. Heliyon 6.4 (2020).

5. Thakur, Sahil, et al. Standalone Highly Efficient Graphene Oxide as an Emerging Visible Light-Driven Photocatalyst and Recyclable Adsorbent for the Sustainable Removal of Organic Pollutants. Langmuir 40.35 (2024): 18486-18502.

6. Avilés-Monreal, Raúl, et al. Degradation of methylene blue catalyzed by a photo-Fenton reaction of $g\text{-}C_3N_4/Fe_3O_4$ nanocomposite with visible light. Fullerenes, Nanotubes and Carbon Nanostructures (2025): 1-14.

7. Wu, Jhen-Yang, et al. Tunable photocatalytic properties of Au-decorated $BiFeO_3$ nanostructures for dye photodegradation. ACS Applied Nano Materials 7.8 (2024): 9777-9788.

8. Rajput, Rekha B., et al. N-doped carbon/$TiO_2$ composites with enhanced photocatalytic performance for the removal of organic pollutants. Journal of Physics and Chemistry of Solids 184 (2024): 111677.

9. Li, Ying, et al. Synthesis of $Co_3O_4/ZnO@$ MG-$C_3N_x$ Catalysts and Their Visible Light Degradation of Methylene Blue Performance. Chinese Journal of Materials Research 39.4 (2025): 241-250.

10. Liu, Huifang, et al. ZnO rod decorated with Ag nanoparticles for enhanced photocatalytic degradation of methylene blue. Journal of Physics and Chemistry of

Solids 129 (2019): 46-53.